Biochimica et Biophysica Acta 1838 (2014) 2404–2411

Contents lists available at ScienceDirect

Biochimica et Biophysica Acta

journal homepage: www.elsevier.com/locate/bbamem

# Measuring localization and diffusion coefficients of basolateral proteins in lateral versus basal membranes using functionalized substrates and kICS analysis

Saw Marlar, Eva C. Arnspang [1], Gitte A. Pedersen, Jennifer S. Koffman, Lene N. Nejsum *

*Institute of Molecular Biology and Genetics and Interdisciplinary Nanoscience Center, Aarhus University, C. F. Moellers Allé 3, Aarhus, Denmark*

ARTICLE INFO

*Article history:*
Received 7 October 2013
Received in revised form 3 June 2014
Accepted 9 June 2014
Available online 17 June 2014

*Keywords:*
(4-6) Diffusion coefficient
kICS: k-space Image Correlation Spectroscopy
Aquaporin
MDCK
Micropatterning

ABSTRACT

Micropatterning enabled semiquantitation of basolateral proteins in lateral and basal membranes of the same cell. Lateral diffusion coefficients of basolateral aquaporin-3 (AQP3-EGFP) and EGFP-AQP4 were extracted from "lateral" and "basal" membranes using identical live-cell imaging and k-space Image Correlation Spectroscopy (kICS).

To simultaneously image proteins in "lateral" and "basal" membranes, micropatterning with the extracellular domain of E-cadherin and collagen, to mimic cell–cell and cell-extracellular matrix (ECM) adhesion, respectively, was used. In kidney collecting duct principal cells AQP3 localizes lateral and basal whereas AQP4 localizes mainly basal. On alternating stripes of E-cadherin and collagen, AQP3-EGFP was predominantly localized to "lateral" compared to "basal" membranes, whereas Orange-AQP4 was evenly distributed. Average diffusion coefficients were extracted via kICS analysis of rapid time-lapse sequences of AQP3-EGFP and EGFP-AQP4 on uniform substrates of either E-cadherin or collagen. AQP3-EGFP was measured to 0.022 ± 0.010 $\mu m^2/s$ on E-cadherin and 0.019 ± 0.004 $\mu m^2/s$ on collagen, whereas EGFP-AQP4 was measured to 0.044 ± 0.009 $\mu m^2/s$ on E-cadherin and 0.037 ± 0.009 $\mu m^2/s$ on collagen, thus, diffusion did not differ between substrates. Cholesterol depletion by methyl-beta-cyclodextrin (MBCD) reduced the AQP3-EGFP diffusion coefficient by 43% from 0.024 ± 0.007 $\mu m^2/s$ (water) to 0.014 ± 0.003 $\mu m^2/s$ (MBCD) ($p < 0.05$) on collagen surfaces, and by 41% from 0.023 ± 0.011 $\mu m^2/s$ (water) to 0.014 ± 0.005 $\mu m^2/s$ (MBCD) ($p < 0.05$) on E-cadherin surfaces. Thus, protein patterning enables the semiquantitation of protein distribution between the "lateral" and "basal" membranes as well as measurements of lateral diffusion coefficients.



## 1. Introduction

An epithelium consists of a layer of cells generating a selective barrier between the exterior and the body. An epithelial cell has three membrane domains: the apical that faces the outside, the lateral which adheres to neighboring cells and the basal which anchors to the extracellular matrix (ECM). The apical and basolateral membranes are separated by tight junctions localized to the apex of the lateral membrane (for reviews, please see [1,2]). Tight junctions secure compartmentalization of plasma membrane proteins and lipids between the apical and basolateral membranes [3], but there are no junctions separating the lateral and basal membranes. Despite the lack of basolateral barrier junctions, membrane proteins may be differentially regulated in the lateral vs. the basal membranes via incorporation into nanodomains/rafts [4–6], alterations in diffusion behavior [7–9] as well as via changes in protein–protein and/or protein–ECM interactions [10,11]. To study protein localization and diffusion in the lateral and basal membranes, different growth conditions as well as imaging techniques have generally been used [12]. To get access to the lateral membrane, epithelial cells are grown on semipermeable filters, on which they generate a tight monolayer. Fluorescently labeled lateral proteins can be imaged using widefield or spinning disk confocal microscopy combined with Fluorescent Recovery After Photobleaching (FRAP) analysis to measure the lateral diffusion [13]. However, when cells are grown on filters, it is not possible to image basal proteins to extract diffusion coefficients, as basal proteins are studied with Total Internal Reflection Fluorescence (TIRF) microscopy, which requires glass coverslips instead of filters [14]. Single particle tracking (SPT) of quantum dot (QD) labeled lateral and basal proteins can be performed with both imaging techniques, however, the label may slow down diffusion especially in the adhering membrane, and moreover, only a fraction of the total pool of proteins is labeled [15–18].

We aimed to set up a system to use identical growth conditions, imaging tools and analysis techniques to investigate the localization and measure lateral diffusion of basolateral membrane proteins in the

* Corresponding author. Tel.: +45 21163121.
*E-mail address:* nejsum@mb.au.dk (L.N. Nejsum).
[1] Present address: National Institutes of Health, Library Drive 18, Bethesda, Maryland 20892, USA.

http://dx.doi.org/10.1016/j.bbamem.2014.06.005
0005-2736/

lateral vs. the basal membranes of epithelial cells. To accomplish this, we studied two aquaporin water channels, AQP3 and AQP4, which are known to localize differently in the basolateral membrane of kidney collecting duct principal cells *in vivo* [19–21].

AQPs [22] are integral water channel proteins widely expressed in plants [23,24], microbes [25,26] and animals [22,27,28]. Most mammalian AQPs are selectively permeable to water while AQP3, −7, −9, and −10 are permeable to both water and glycerol (for review, please see [28]). Besides kidney, AQP3 is expressed in the basolateral membrane of many epithelial cells in different organs including lung [29], skin [30,31], eye [32] and colon [33], and AQP4 is heavily expressed in brain [33,34] as well as kidney [20]. In the kidney collecting duct, urine concentration is fine-tuned in response to the antidiuretic hormone arginine vasopressin (AVP) [35]. AVP binding to the basolateral AVP receptor 2 (AVPR2) in collecting duct principal cells, initiates a signaling cascade leading to apical insertion of AQP2 containing vesicles [36], thereby increasing water permeability of the apical membrane. This leads to increased water uptake and subsequent urine concentration [37–39]. AQP3 and AQP4 are both expressed in the basolateral membrane of collecting duct principal cells [19,20] and are thought to facilitate exit of water, which entered via apically localized AQP2.

AQP3 null mice suffer from nephrogenic diabetes insipidus (NDI) [40], which is the inability to concentrate urine in response to AVP, whereas AQP4 null mice only have a mild concentration defect [41]. Double knockout of both AQP3 and AQP4 enhanced the concentration defect of single AQP3 knockout in mice, indicating a compensatory mechanism between AQP3 and AQP4 [40]. Although AQP3 and AQP4 are homologous proteins and serve similar functions in the collecting duct concentrating mechanism, they are differentially localized within the basolateral membrane. AQP3 is present in both the basal and lateral membrane domains of collecting duct principal cells in rat [19,21], whereas AQP4 is localized predominantly in the basal membrane domain [20,21]. It is unknown why these two homologous proteins with similar function are differently localized in the basal and lateral membrane domains. To study AQP3 and AQP4 plasma membrane localization in a cell system, patterning of 10 μm-wide alternating stripes of E-cadherin:Fc and collagen IV, mimicking a lateral membrane of a neighboring cell and basal lamina, respectively, was performed on two-dimensional glass surfaces by the use of microcontact printing and biochemical functionalization [42,43]. This approach has previously been used to study integrin- and E-cadherin-mediated adhesions during epithelial cell migration [43] and a checker box patterning approach with the same proteins has been used to visualize docking of basolateral post-Golgi carriers [44]. Those studies focused on proteins directly interacting with the presented substrates, however, this study is the first to use this technique to investigate plasma membrane localization and regulation of basolateral transport proteins not involved in cell adhesion.

Upon cell adhesion to the patterns, the plasma membrane remodels into stripes resembling “lateral” and “basal” membranes enabling visualization of fluorescently tagged basolateral proteins using spinning disk or TIRF microscopy. Moreover, homogeneous patterns were used to measure the average lateral diffusion coefficient of AQP3 in either the “lateral” (E-cadherin:Fc coated) or the “basal” (collagen coated) membranes using spinning disk microscopy and TIRF microscopy followed by a novel analysis technique, kICS, which calculates the average diffusion coefficient of the total pool of fluorescent proteins [45–47]. This showed that AQP3-EGFP and Orange-AQP4 were differentially localized in the “lateral” and “basal” membrane domains within the same cell and that diffusion coefficients of AQP3-EGFP and EGFP-AQP4 did not change between “lateral” and “basal” membranes.

Thus, combining E-cadherin:Fc and collagen substrates with spinning disk or TIRF microscopy and subsequent kICS analysis enables qualitative and quantitative analysis of plasma membrane proteins in “lateral” vs. “basal” membranes.

## 2. Materials and methods

### 2.1. Cell culture

MDCK GII cells [48,49] were cultured in DMEM with low glucose (1 g/L, Gibco) supplemented with 10% fetal bovine serum (FBS, Gibco or Atlas) and 0.5 U/mL penicillin (Sigma), 0.5 g/mL streptomycin (Gibco), 1 mg/mL kanamycin (Gibco) (1% PSK), and maintained at 37 °C and 5% $CO_2$. Cells were transfected with AQP3-EGFP, or EGFP-AQP4 (gifts from Dr. Anita Aperia, Karolinska Institute, Sweden), or a combination of AQP3-EGFP and Orange-AQP4 [50] using Effectene (Qiagen) or Lipofectamine2000 (Invitrogen). AQP4 was the full length version, which without the expression of the M23 version, does not form arrays in the membrane [51]. For the selection of stable cell lines, selection with G418 (Gibco) was carried out. Stable clones were analyzed for expression and localization by microscopy, and protein size was confirmed by Western blotting using a rabbit anti-GFP antibody (Abcam), an AQP4 antibody (Alomone) or an AQP3 antibody (Provided by the Water and Salt Research Center, AU, DK). The AQP4 clone was submitted to fluorescence-activated cell sorting (FACS) to increase the number of expressing cells. All constructs were stably expressed in MDCK GII cells without any apparent change in phenotype. Orange-AQP4 was generated by the subcloning of AQP4 into Clontech vectors containing EGFP-C1 Clontech vector constructed to contain Orange (a gift from Dr. Roger Tsien) instead of EGFP.

### 2.2. Micropattern generation

#### 2.2.1. Expression and purification of E-cadherin:Fc

HEK 293 cells recombinantly expressing an E-cadherin:Fc plasmid composed of the extracellular domain of canine E-cadherin fused to the Fc domain of human IgG1 were kindly donated by W. James Nelson [42]. HEK293-Ecadherin:Fc cells were seeded in a cell factory (Nunc) for large-scale production of secreted E-cadherin:Fc proteins. When the cells were approximately 75% confluent they were washed 3 times in DMEM and incubated for 1 h in the third wash to remove traces of FBS. The cells were then incubated for further 2 days in DMEM without serum to allow the expression and secretion of E-cadherin:Fc before the media was harvested. To remove cell debris and aggregates the media was filtered through a 0.22 μm pore-sized filter and a complete mini protease inhibitor cocktail (Roche) was added to prevent degradation of proteins.

The media was applied onto a HiTrap Protein A HP column (GE Healthcare) that had been equilibrated in 20 mM sodium phosphate pH 7.2 at 4 °C using a flow rate of 1 mL/min. Purified E-cadherin:Fc was eluted from the column using 0.1 M glycine pH 2.6 and immediately neutralized using NaOH to a pH of approximately 7. Eluted proteins were buffer-shifted into Ringer's buffer (10 mM HEPES pH 7.4, 154 mM NaCl, 7.2 mM KCl) and concentrated using Pierce® Concentrators with a molecular-weight cutoff of 9 kDa. Protein concentration and purity were evaluated by SDS-PAGE and Coomassie brilliant blue staining using bovine serum albumin (BSA) as a protein standard.

#### 2.2.2. Protein substrates

Micropatterns were generated using a standard protocol of microcontact printing and biochemical functionalization [43]. The method involves two main steps: 1) preparation of glass surfaces to form chemical binding sites by silanization, and 2) fabrication of the E-cadherin:Fc and collagen substrates. Glass coverslips were thoroughly cleaned in methanol followed by a 5-minute exposure to plasma (Diener plasma cleaner). A reactive surface was generated by silanization. Collagen IV (Sigma) was labeled with Cy3.5 using a fluorescence labeling kit (Amersham) according to manufacturer's protocol. Labeled collagen was added to polydimethylsiloxane (PDMS) stamps containing 10 μm-wide stripes followed by microstamping onto the silanized coverslip. Non-stamped surfaces of coverslips were sequentially incubated with

solutions of EZ-link Sulfo-NHS-LC-Biotin (Thermo Scientific), Neutravidin (Thermo Scientific) and biotinylated protein A (Thermo Scientific) for correct localization and orientation of the E-cadherin:Fc. Following blocking with D-biotin dissolved in dimethyl sulfoxide (DMSO), coverslips were incubated with purified E-cadherin:Fc generating a pattern of 10 μm-wide alternating stripes of unlabeled E-cadherin:Fc and Cy3.5-labeled collagen [42,43]. Micropatterns were prepared and used fresh for localization studies. For diffusion measurement, coverslips were uniformly coated either with E-cadherin:Fc or with collagen, stored in PBS and used within a week.

### 2.3. Microscopy

For live cell TIRF microscopy of AQP3-EGFP and Orange-AQP4, cells were seeded at subconfluency on patterns (see above) for at least one hour before imaging. For imaging, media was changed to phenol red-free DMEM (Sigma-Aldrich) with 10% FBS (Atlas) and 25 mM HEPES (Invitrogen) and cells were imaged using the Marianas system (Intelligent Imaging Innovations) with a microscope (Axiovert 200 M; Carl Zeiss MicroImaging, Inc.) equipped with a camera (Photometrics CoolSNAP; Rober Scientific) and a TIRF system (TIRF Slider; Carl Zeiss MicroImaging, Inc.). For live cell Spinning Disk microscopy of AQP3-EGFP, cells were seeded at subconfluency on coated coverslips (see above) the day before imaging. For imaging, media was changed to phenol red-free DMEM (Sigma-Aldrich) with 10% FBS, 1% PSK and 25 mM HEPES. Cells were pre-treated with 5 mM methyl-beta-cyclodextrin (MBCD, stock was 100 mM) to deplete cholesterol in parallel to water. Cells were imaged using a Nikon Ti Eclipse microscope equipped with a Yokogawa CSU-X1 spinning disk unit, Andor Laser launcher and an Andor iXon + EMCCD for detection. Imaging was performed at 35 °C using a 491 nm laser line for excitation. Imaging was performed with focus set close to the plasma membrane, and a 60× Plan Apo oil objective (NA 1.40) was used. Stacks composed of 500 frames were acquired with 40 ms integration time at an average frame rate of 9.15 Hz. For live cell TIRF microscopy of EGFP-AQP4, cells were seeded on functionalized substrates (as for AQP3-EGFP) and imaging was carried out using a Nikon Ti Eclipse microscope equipped with a motorized TIRF unit, a Perfect Focus 3 system, a CFI60 Apo TIRF 100× objective (NA1.49) and an Andor Zyla sCMOS for detection. Imaging was performed at 37 °C with a 488 nm laser line for excitation. Stacks containing 500 frames were acquired at 10 Hz. Images were analyzed using Slidebook (Intelligent Imaging Innovations) or ImageJ (available at http://rsb.info.nih.gov/ij) software [52].

### 2.4. Measurement of diffusion coefficients by kICS analysis

Image stacks were imported into ImageJ [52] and crops including no moving membrane, holes or moving cell organelles, were selected. The crops were analyzed using the kICS code in MATLAB [45]. For all crops the same settings were used. For the quantitation of AQP3-EGFP diffusion, the maximum number of time lags ($\tau$) was set to 6 and the maximum $k^2$ value was set to 16. Whereas EGFP-AQP4 diffusion was calculated using the maximum $\tau$ of 7 and the maximum $k^2$ value of 30. The diffusion coefficients were imported into Excel, and averaged over all crops, 8–23 crops from 5 to 23 cells per condition. Obvious out layers were removed. Thereafter, an average diffusion plot of different conditions was generated. The number of crops had a large impact on the standard deviations, thus, in the experiments were fewer good cells were available, the standard deviations are largest.

### 2.5. Statistics

Values are presented as means ± STDEV. Comparisons between groups were made by unpaired *t*-test. p-values $< 0.05$ were considered significant.

## 3. Results and discussion

### 3.1. AQP3 accumulated at E-cadherin:Fc stripes

AQP3 and AQP4 both serve as basolateral exit pathways for water reabsorbed in collecting duct principal cells via apically localized AQP2. Although AQP3 and AQP4 are homologous proteins with similar functions, the subcellular localization seems to be differently regulated in collecting duct principal cells *in vivo*. AQP3 is found to be abundant in both the lateral and basal plasma membranes of collecting duct principal cells in rat [19,21], whereas AQP4 is predominantly expressed in the basal membrane [20,21]. This phenomenon of spatial segregation of homologous transport proteins in the same membrane domain has never been studied due to the lack of a model system. For simultaneous detection of fluorescent proteins in the "lateral" and "basal" membranes in the same cell, a micropatterning approach of alternating stripes of E-cadherin:Fc and collagen to mimic lateral and basal membranes, respectively [43], combined with TIRF microscopy was used.

To study the localization of AQP3 and AQP4 in the "lateral" and "basal" membranes, cells stably expressing AQP3-EGFP and Orange-AQP4 [50] were seeded onto the patterns and imaged using live-TIRF microscopy. TIRF images clearly showed that AQP3-EGFP accumulated to a greater extent in membranes resembling "lateral" (E-cadherin:Fc) compared to "basal" (collagen), whereas there was no noticeable difference in Orange-AQP4 accumulation between the two different membrane domains (Fig. 1, A). This was confirmed by semiquantification, which showed that the ratio of AQP3-EGFP signal on E-cadherin:Fc stripes in relation to collagen was 1.27 ± 0.10, whereas Orange-AQP4 was evenly distributed on E-cadherin:Fc (1.05 ± 0.08) compared to collagen (Fig. 1, B). This indicates that membrane abundance of AQP3 and AQP4 is indeed regulated in the lateral and basal membranes within the same cell. Compared to the even distribution of Orange-AQP4, the accumulation of AQP3-EGFP on E-cadherin:Fc stripes suggests a retention mechanism of AQP3-EGFP in "lateral" membranes. Since AQP3 and AQP4 accumulate differently between the lateral and basal membranes in vivo, and also localize differently on stripes of "lateral" and "basal" membranes, there may be different regulatory mechanisms, which control plasma membrane density of the two proteins. Adhesion proteins are expected to segregate in the basolateral membrane, where E-cadherins mediate lateral cell–cell adhesion and integrins mediate cell-ECM adhesion [42,43]. However, it is surprising that two homologous proteins with no known participation in cell adhesion and which serve similar functions, also segregate in the "lateral" and "basal" membranes.

### 3.2. Diffusion rates are similar in the "lateral" and "basal" plasma membranes

AQP3 accumulation in "lateral" membranes compared to "basal" indicates different modes of regulation between the two domains. Since different modes of regulation like protein–protein, protein–lipid interactions as well as membrane crowding can alter lateral diffusion of proteins [9,11], AQP3-EGFP diffusion coefficients in the "lateral" and "basal" domains were measured. To image and analyze AQP3-EGFP diffusion coefficients in the "lateral" and the "basal" membranes identically, uniform coatings of either E-cadherin:Fc or collagen were used. Image acquisitions were performed with a spinning disk microscope with focus set to the basolateral membrane followed by kICS analysis. kICS is a novel analysis method [45–47], which following 2D Fourier transform to reciprocal (k-) space, correlates fluorescence microscopy image sequences. The technique can be used to measure number density, velocity and diffusion coefficients of fluorescence-tagged and dye/QD-labeled proteins while being uninfluenced by probe photophysics i.e. QD blinking [18,46,47]. This technique requires a fairly large membrane area and thus, for diffusion measurements, even surfaces of either E-cadherin:Fc or collagen were generated. Previously, diffusion coefficients of plasma membrane proteins in the lateral membrane were calculated by FRAP analysis of cells grown on semipermeable filters or

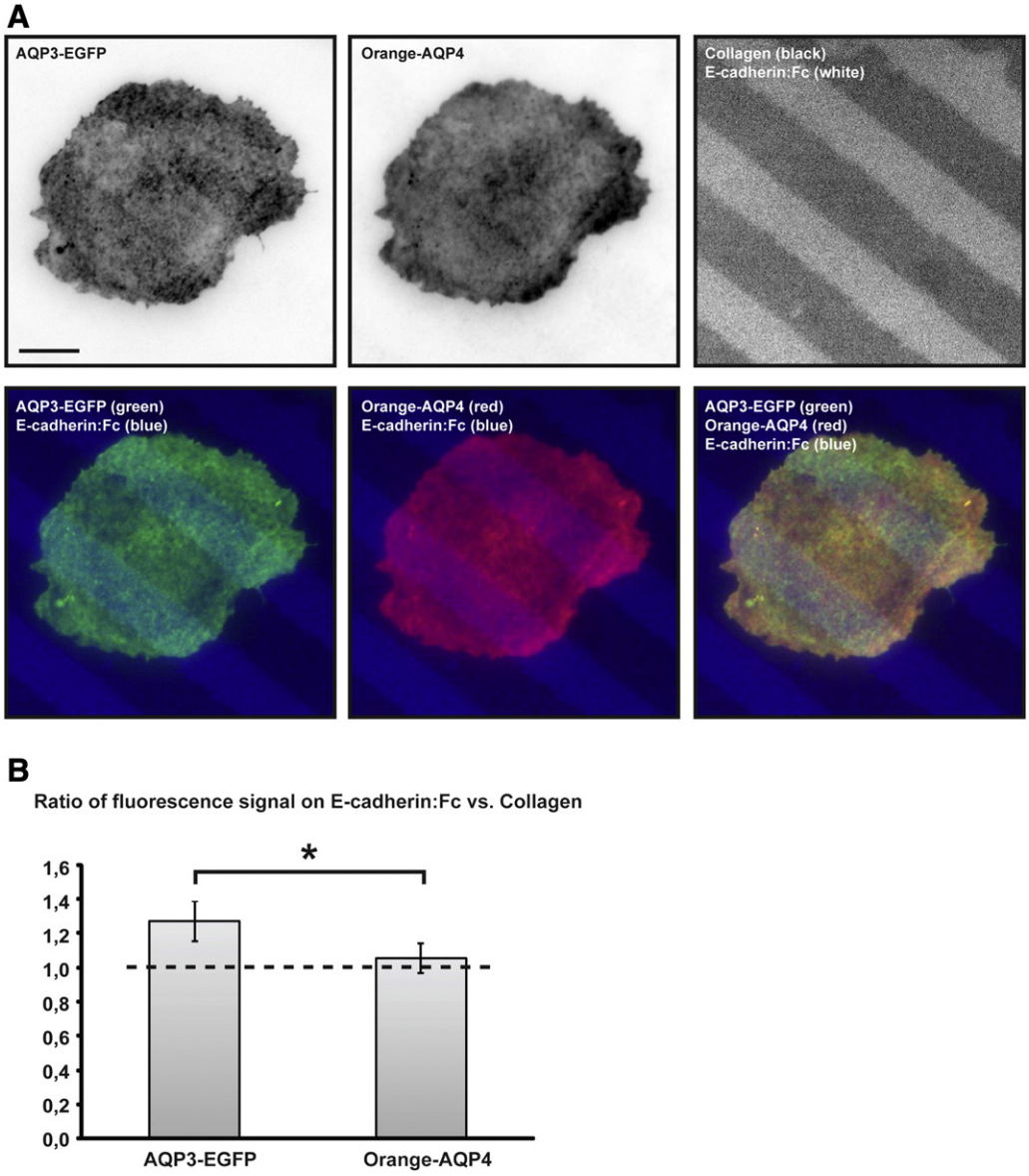


**Fig. 1.** AQP3-EGFP accumulates in "lateral" membranes at E-cadherin:Fc stripes. (A) Total internal reflection fluorescence (TIRF) images of live MDCK cell stably expressing AQP3-EGFP and Orange-AQP4 on E-cadherin:Fc vs. collagen stripes. Top panel shows single channels of original fluorescence intensity signals in inverted contrast. Left: AQP3-EGFP, middle: Orange-AQP4 and right: E-cadherin:Fc stripes (collagen was unlabeled). Bottom panel shows merged images: left: AQP3-EGFP (green) and stripes (E-cadherin:Fc stripes are blue, collagen black), middle: Orange-AQP4 (red) and stripes (E-cadherin:Fc stripes are blue, collagen black) and left: AQP3-EGFP (green), Orange-AQP4 (red) and stripes (E-cadherin:Fc stripes are blue, collagen black). (B) Ratio of fluorescence signal of AQP3-EGFP and Orange-AQP4 on E-cadherin:Fc vs. collagen. Data show mean ± SEM. *$p < 0.05$.

glass [7], whereas the diffusion of basolateral proteins could be calculated from FRAP using TIRF or spinning disk confocal microscopy [13,14]. FRAP analysis is powerful to investigate the recovery of a protein following photobleaching and can thus be used to extract diffusion coefficients [53]. kICS enables the extraction of an average diffusion coefficient of the total pool of labeled proteins at the plasma membrane [45] without the need to distinguish single particles or individual trajectories, without the need to perform photobleaching, and is probe and labeling density independent.

The steady state diffusion coefficient of AQP3-EGFP in the "lateral" membrane was measured to 0.022 ± 0.010 $\mu m^2/s$ compared to 0.019 ± 0.004 $\mu m^2/s$ in the "basal" membrane (Fig. 2, A and B), and thus, there was no difference in the diffusion of AQP3-EGFP between the membrane domains. TIRF microscopy and subsequent kICS analysis revealed that EGFP-AQP4 diffusion did not vary between the lateral and basal membranes, 0.044 ± 0.009 $\mu m^2/s$ on E-cadherin:Fc and 0.037 ± 0.009 $\mu m^2/s$ on collagen (Fig. 2, C + D). Hence, there was no difference in diffusion coefficients of the two proteins between "lateral" and "basal" membranes. The higher diffusion coefficient of EGFP-AQP4 compared to AQP3-EGFP may be due to the higher temperature during imaging acquisition. AQP3 and AQP4 experiments were done on different microscope setups. It cannot be excluded that different imaging methods may yield slightly different diffusion measurements. Therefore, it is important to only compare data obtained on the same microscope setup. Measurements were done on subconfluent non-polarized cells as polarization of cells on semipermeable filters does not allow imaging of protein diffusion in the basal membrane. AQP3 diffusion in vivo may be different than the diffusion measured in cells, since the diffusion of membrane proteins and lipids varies even between cell types as well as between confluent and sub-confluent cells [54,55]. Lipid diffusion is

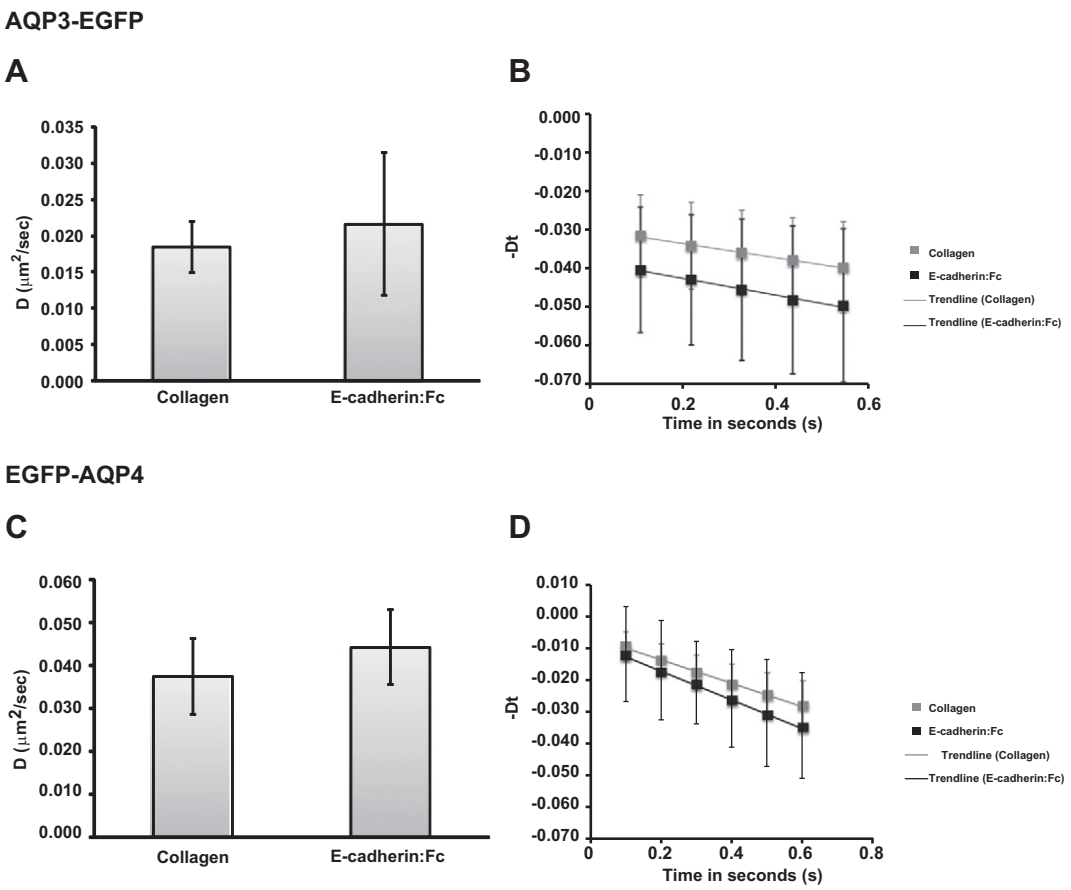


**Fig. 2.** Representative diffusion coefficients of AQP3-EGFP and EGFP-AQP4 on E-cadherin:Fc and collagen surfaces. (A + C) Graphs show the average steady state diffusion coefficients of AQP3-EGFP (A), and EGFP-AQP4 (C) on uniform surfaces of E-cadherin:Fc and collagen. Data show mean ± STDEV. (B + D) Diffusion plots for AQP3-EGFP (B), and EGFP-AQP4 (D) showing −Dt, the diffusion coefficient D and time t versus the time in seconds. The gray line represents collagen, the black line E-cadherin:Fc. The plot was generated by averaging over all data for each time point giving an average diffusion plot. The slope of the line is minus the diffusion coefficient, hence, equal diffusion coefficients result in parallel lines and different diffusion coefficients result in non-parallel lines.

increased in polarized compared to subconfluent MDCK cells [54], whereas, AQP1 diffused faster in non-polarized COS-7 cells compared to confluent MDCK cells [55].

### 3.3. Cholesterol depletion altered AQP3-EGFP diffusion in the "lateral" and "basal" membranes

Several lines of evidence suggest that plasma membranes contain microdomains/lipid rafts rich in spingolipids and cholesterol [56,57], which selectively accommodate proteins responsible for cellular signaling [58–60], protein trafficking [61,62] and plasma membrane turnover [63,64]. Also, it has been shown for many proteins that cholesterol depletion slows down lateral diffusion [65,66]. Some mammalian AQPs such as AQP0 [67], AQP1 [68,69] and AQP3-5 [70–72] are found to associate with rafts in different mammalian cell types. In keratinocytes, AQP3 is found in caveolin-rich microdomains as part of a signaling module [70], and thus, rafts may be essential for AQP3 plasma membrane diffusion, and disruption may thus result in decreased diffusion coefficients of AQP3-EGFP.

Cells were pre-treated with MBCD to deplete cholesterol in parallel to water (control) and subjected to rapid time-lapse spinning disk imaging of AQP3-EGFP followed by kICS analysis. Cholesterol depletion reduced the diffusion coefficient of AQP3-EGFP by 43% from 0.024 ± 0.007 $\mu m^2/s$ (water) to 0.014 ± 0.003 $\mu m^2/s$ (MBCD) ($p < 0.05$) (Fig. 3) in the "basal" plasma membrane. A similar effect of MBCD was found in the "lateral" membrane where the diffusion coefficient of AQP3-EGFP decreased by 41% from 0.023 ± 0.011 $\mu m^2/s$ (water) to 0.014 ± 0.005 $\mu m^2/s$ (MBCD) ($p < 0.05$) (Fig. 3). All diffusion data are summarized in Table 1. These data indicate that lipid dispersion, triggered by cholesterol depletion decreases lateral diffusion of AQP3-EGFP. As AQP3 is found in caveolin-rich microdomains [70], it is possible that lipid rafts are involved in AQP3 diffusion in both the lateral and basal membranes, however, this is speculative. Furthermore, the addition of water at a 20× dilution was found to cause a slight increase in the average diffusion coefficients of AQP3-EGFP compared to the values measured in the baseline test, on both the E-cadherin:Fc and collagen surfaces, indicating an influence of media osmolality on the lateral diffusion of AQP3-EGFP.

A similar reduction in diffusion of AQP1 was found upon cholesterol depletion in COS7 cells and MDCK cells via SPT approach [55]. Similarly, MBCD was found to slow down lateral diffusion of human leukocyte antigen (HLA) molecules in fibroblasts, calculated by FRAP, in a manner dependent on F-actin reorganization [73]. It is therefore assumed that lipid dispersion may lead to the formation of network-like structures, which act as barriers in the plane of the plasma membrane and thus restrict lateral diffusion of proteins [74]. Thus, the effect of MBCD may be a general effect on plasma membrane proteins and also the effect may be similar in the basal and lateral membranes.

AQP3 compartmentalization has yet to be tested by an advanced imaging system such as super resolution microscopy. Since AQP3 is widely expressed in different organs and cell types of the body, the effect of MBCD may also vary among cell types.

Technically, FRAP and SPT approaches are widely used to measure diffusion coefficients of fluorescence tagged/fluorophore-labeled proteins (for review please see [75]). In this study, kICS [45–47] analysis was applied In FRAP, a small area of interest is bleached and the rate

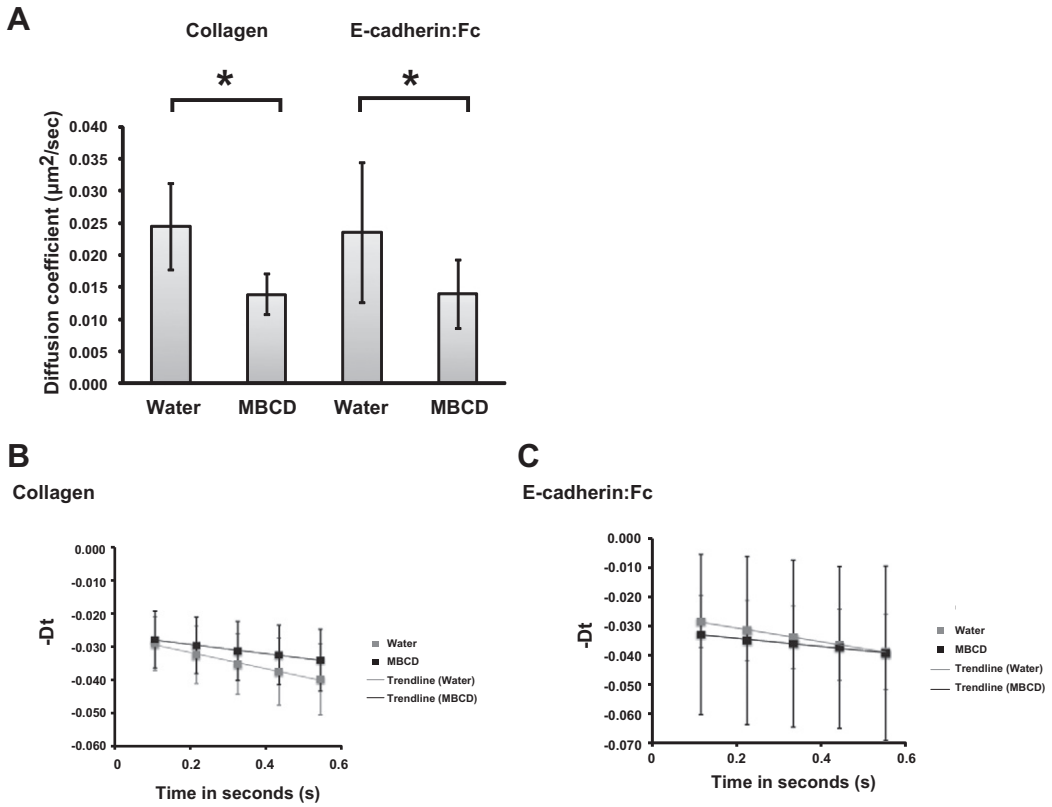


**Fig. 3.** Cholesterol depletion decreases diffusion coefficients of AQP3-EGFP on both E-cadherin:Fc and collagen substrates. (A) Graph shows the average diffusion coefficients of AQP3-EGFP on uniform surfaces of E-cadherin:Fc and collagen upon water (control) and 5 mM MBCD treatments. Data show mean ± STDEV, *$p < 0.05$; (B + C) Diffusion plots for AQP3-EGFP on uniform surfaces of collagen (B) and E-cadherin:Fc (C) upon water (control) and 5 mM MBCD treatments showing −Dt, the diffusion coefficient D and time t versus the time in seconds. The gray line represents water addition, the black line MBCD. The plot was generated by averaging over all data for each time point giving an average diffusion plot. The slope of the line is minus the diffusion coefficient, hence, equal diffusion coefficients result in parallel lines and different diffusion coefficients result in non-parallel lines.

of fluorescence recovery of the area is measured as diffusion of the protein. Partial recovery of the bleached area, stationary fraction of proteins as well as reversible photobleaching are concerns in the practical application of FRAP [53]. In contrast, SPT analysis provides not only diffusion coefficients but also protein trajectories. However, SPT technique requires labeling of proteins with a fluorophore at an extracellular tag, which, in some cases, perturbs folding and localization of the protein [15,75]. In addition, the presence of the tag coupled to a probe at the cell surface may hinder the binding between cell–cell and cell–ECM when measuring diffusion of adhesive proteins [76]. Although it is possible to have QDs on the adhering membranes, the diffusion might be slowed down due to the presence of bulky QD-antibody nanobio composites [15,18]. Labeling is also limited to a small fraction of the membrane proteins, which may not represent the activity of the entire pool of plasma membrane proteins. Besides, the technique is often regarded as a time-consuming process as hundreds of trajectories need to be analyzed to get statistically reliable data. Complementary to FRAP and SPT, kICS analysis is an alternative tool to extract dynamic parameters of plasma membrane proteins [45]. The steady state diffusion coefficient of EGFP-AQP4 measured using kICS was 0.037 ± 0.009 $\mu m^2/s$ on collagen and 0.044 ± 0.009 $\mu m^2/s$ on E:cadherin:Fc, which is highly consistent with the previously reported diffusion coefficient of the same protein, ~0.052 $\mu m^2/s$, in COS-7 cells measured by SPT analysis [77]. Using FRAP, Umenishi et al. (2000) also reported the diffusion coefficient of apical AQP2 in LLC-PK1 cells, ~0.009 $\mu m^2/s$, which was an order of magnitude smaller than that of AQP4 described above [7]. These data further confirm the compatibility of kICS with FRAP and SPT, which are widely applied in diffusion measurements. Compatibility of kICS with conventional SPT analysis has recently been shown in the method validation study by Arnspang et al. [46].

**Table 1**
Summary of diffusion coefficients on collagen and E-cadherin:Fc substrates.

| Diffusion coefficients ($\mu m^2/s$) | Collagen | E-cadherin:Fc |
|---|---|---|
| AQP3-EGFP (35 °C) | 0.019 ± 0.004 | 0.022 ± 0.010 |
| EGFP-AQP4 (37 °C) | 0.037 ± 0.009 | 0.044 ± 0.009 |
| AQP3-EGFP — water (35 °C) | 0.024 ± 0.007 | 0.023 ± 0.011 |
| AQP3-EGFP — MBCD (35 °C) | 0.014 ± 0.003 | 0.014 ± 0.005 |

## 4. Conclusions

Protein patterning enabled semiquantitation of fluorescently labeled transport proteins, here AQP3-EGFP and Orange-AQP4, in the "lateral" vs. the "basal" membranes. Combining protein substrates with high-speed imaging and kICS analysis enabled the extraction of diffusion coefficients of fluorescently tagged plasma membrane proteins in the "lateral" and "basal" plasma membranes. AQP3-EGFP accumulated to a higher degree in "lateral" membranes compared to Orange-AQP4, which was evenly distributed. Steady state diffusion of AQP3-EGFP as well as cholesterol sensitivity was identical on both the E-cadherin:Fc and collagen surfaces. Likewise, EGFP-AQP4 displayed identical diffusion between the E-cadherin:Fc and collagen substrates. Future studies will be needed to clarify the underlying molecular mechanism of spatio-temporal regulation of AQP3 and AQP4 between the lateral and basal membranes.

## Acknowledgements

We thank Dr. Anita Aperia (Karolinska Institute, Sweden) for AQP3-EGFP and EGFP-AQP4 and Dr. Roger Tsien (University of California San

Diego) for the Orange containing plasmids. We thank Dr. W. James Nelson for the cell line secreting E-cadherin:Fc and the Water and Salt Research Center for AQP3 antibodies. We also thank Nicolas Borghi for much help with generating the patterns. This work was supported by a post doctoral fellowship to LNN and subsequently a Lundbeck Junior Group Leader Fellowship to LNN from the Lundbeck Foundation, and funding from the Graduate School of Science and Technology (GSST), AU, to SM, as well as a Sapere Aude stage 1 fellowship from the Danish National Research Foundation to ECA. The TIRF microscope was funded by MEMBRANES (Aarhus University, Denmark), the Lundbeck Foundation and the Carlsberg Foundation. We also thank the Danish Molecular Bioimaging Center at University of Southern Denmark for the access to spinning disk microscopy.

## References

[1] J. Chen, M. Zhang, The Par3/Par6/aPKC complex and epithelial cell polarity, Exp. Cell Res. 319 (2013) 1357–1364.
[2] K. Matter, M.S. Balda, Signalling to and from tight junctions, Nat. Rev. Mol. Cell Biol. 4 (2003) 225–236.
[3] G. Vanmeer, K. Simons, The function of tight junctions in maintaining differences in lipid-composition between the apical and the basolateral cell-surface domains of Mdck cells, EMBO J. 5 (1986) 1455–1464.
[4] H.T. He, D. Marguet, Detecting nanodomains in living cell membrane by fluorescence correlation spectroscopy, Annu. Rev. Phys. Chem. 62 (2011) 417–436.
[5] A.D. Douglass, R.D. Vale, Single-molecule microscopy reveals plasma membrane microdomains created by protein–protein networks that exclude or trap signaling molecules in T cells, Cell 121 (2005) 937–950.
[6] M. Sharma, J. Celver, J.C. Octeau, A. Kovoor, Plasma membrane compartmentalization of D2 dopamine receptors, J. Biol. Chem. 288 (2013) 12554–12568.
[7] F. Umenishi, J.M. Verbavatz, A.S. Verkman, cAMP regulated membrane diffusion of a green fluorescent protein-aquaporin 2 chimera, Biophys. J. 78 (2000) 1024–1035.
[8] D.A. Richards, V. De Paola, P. Caroni, B.H. Gahwiler, R.A. McKinney, AMPA-receptor activation regulates the diffusion of a membrane marker in parallel with dendritic spine motility in the mouse hippocampus, J. Physiol. 558 (2004) 503–512.
[9] M. Javanainen, H. Hammaren, L. Monticelli, J.H. Jeon, M.S. Miettinen, H. Martinez-Seara, R. Metzler, I. Vattulainen, Anomalous and normal diffusion of proteins and lipids in crowded lipid membranes, Faraday Discuss. 161 (2013) 397–417 (discussion 419-359).
[10] D. Hoshino, N. Koshikawa, T. Suzuki, V. Quaranta, A.M. Weaver, M. Seiki, K. Ichikawa, Establishment and validation of computational model for MT1-MMP dependent ECM degradation and intervention strategies, PLoS Comput. Biol. 8 (2012) e1002479.
[11] C.G. Specht, N. Grunewald, O. Pascual, N. Rostgaard, G. Schwarz, A. Triller, Regulation of glycine receptor diffusion properties and gephyrin interactions by protein kinase C, EMBO J. 30 (2011) 3842–3853.
[12] S.A. Kim, H. Sanabria, M.A. Digman, E. Gratton, P. Schwille, W.R. Zipfel, M.N. Waxham, Quantifying translational mobility in neurons: comparison between current optical techniques, J. Neurosci. 30 (2010) 16409–16416.
[13] H. Deschout, J. Hagman, S. Fransson, J. Jonasson, M. Rudemo, N. Loren, K. Braeckmans, Straightforward FRAP for quantitative diffusion measurements with a laser scanning microscope, Opt. Express 18 (2010) 22886–22905.
[14] I. Marki, M. Leutenegger, M. Geissbuehler, R. Robelek, E.K. Sinner, T. Lasser, Imaging of G protein-coupled receptors in solid-supported planar membranes at the single molecule level, Proc. SPIE 6862 (2008).
[15] K. Murase, T. Fujiwara, Y. Umemura, K. Suzuki, R. Iino, H. Yamashita, M. Saito, H. Murakoshi, K. Ritchie, A. Kusumi, Ultrafine membrane compartments for molecular diffusion as revealed by single molecule techniques, Biophys. J. 86 (2004) 4075–4093.
[16] V. Nechyporuk-Zloy, P. Dieterich, H. Oberleithner, C. Stock, A. Schwab, Dynamics of single potassium channel proteins in the plasma membrane of migrating cells, Am. J. Physiol. Cell Physiol. 294 (2008) C1096–C1102.
[17] L. Groc, M. Heine, L. Cognet, K. Brickley, F.A. Stephenson, B. Lounis, D. Choquet, Differential activity-dependent regulation of the lateral mobilities of AMPA and NMDA receptors, Nat. Neurosci. 7 (2004) 695–696.
[18] S. Marlar, E.C. Arnspang, J.S. Koffman, E.M. Locke, B.M. Christensen, L.N. Nejsum, Elevated cAMP increases aquaporin-3 plasma membrane diffusion, Am. J. Physiol. Cell Physiol. 306 (6) (2014 Mar 15) C598–606, http://dx.doi.org/10.1152/ajpcell.00132.2013 Epub 2014 Jan 22.
[19] C.A. Ecelbarger, J. Terris, G. Frindt, M. Echevarria, D. Marples, S. Nielsen, M.A. Knepper, Aquaporin-3 water channel localization and regulation in rat kidney, Am. J. Physiol. 269 (1995) F663–F672.
[20] J. Terris, C.A. Ecelbarger, D. Marples, M.A. Knepper, S. Nielsen, Distribution of aquaporin-4 water channel expression within rat kidney, Am. J. Physiol. Renal Fluid Electrolyte Physiol. 269 (1995) F775–F785.
[21] D. Marples, J. Frokiaer, S. Nielsen, Long-term regulation of aquaporins in the kidney, Am. J. Physiol. 276 (1999) F331–F339.
[22] G.M. Preston, T.P. Carroll, W.B. Guggino, P. Agre, Appearance of water channels in xenopus oocytes expressing red-cell CHIP28 protein, Science 256 (1992) 385–387.
[23] C. Maurel, J. Reizer, J.I. Schroeder, M.J. Chrispeels, The vacuolar membrane protein gamma-TIP creates water specific channels in Xenopus oocytes, EMBO J. 12 (1993) 2241–2247.
[24] R. Kaldenhoff, M. Fischer, Aquaporins in plants, Acta Physiol. (Oxf.) 187 (2006) 169–176.
[25] M. Bonhivers, J.M. Carbrey, S.J. Gould, P. Agren, Aquaporins in Saccharomyces — genetic and functional distinctions between laboratory and wild-type strains, J. Biol. Chem. 273 (1998) 27565–27572.
[26] S. Hohmann, R.M. Bill, G. Kayingo, B.A. Prior, Microbial MIP channels, Trends Microbiol. 8 (2000) 33–38.
[27] E. Kruse, N. Uehlein, R. Kaldenhoff, The aquaporins, Genome Biol. 7 (2006) 206.
[28] L.S. King, D. Kozono, P. Agre, From structure to disease: the evolving tale of aquaporin biology, Nat. Rev. Mol. Cell Biol. 5 (2004) 687–698.
[29] S. Nielsen, L.S. King, B.M. Christensen, P. Agre, Aquaporins in complex tissues. II. Subcellular distribution in respiratory and glandular tissues of rat, Am. J. Physiol. 273 (1997) C1549–C1561.
[30] T. Matsuzaki, T. Suzuki, H. Koyama, S. Tanaka, K. Takata, Water channel protein AQP3 is present in epithelia exposed to the environment of possible water loss, J. Histochem. Cytochem. 47 (1999) 1275–1286.
[31] L.N. Nejsum, T.H. Kwon, U.B. Jensen, O. Fumagalli, J. Frokiaer, C.M. Krane, A.G. Menon, L.S. King, P.C. Agre, S. Nielsen, Functional requirement of aquaporin-5 in plasma membranes of sweat glands, Proc. Natl. Acad. Sci. U. S. A. 99 (2002) 511–516.
[32] S. Hamann, T. Zeuthen, M. La Cour, E.A. Nagelhus, O.P. Ottersen, P. Agre, S. Nielsen, Aquaporins in complex tissues: distribution of aquaporins 1-5 in human and rat eye, Am. J. Physiol. 274 (1998) C1332–C1345.
[33] A. Frigeri, M.A. Gropper, C.W. Turck, A.S. Verkman, Immunolocalization of the mercurial-insensitive water channel and glycerol intrinsic protein in epithelial cell plasma membranes, Proc. Natl. Acad. Sci. U. S. A. 92 (1995) 4328–4331.
[34] H. Hasegawa, T. Ma, W. Skach, M.A. Matthay, A.S. Verkman, Molecular cloning of a mercurial-insensitive water channel expressed in selected water-transporting tissues, J. Biol. Chem. 269 (1994) 5497–5500.
[35] T.L. Pannabecker, Comparative physiology and architecture associated with the mammalian urine concentrating mechanism: role of inner medullary water and urea transport pathways in the rodent medulla, Am. J. Physiol. Regul. Integr. Comp. Physiol. 304 (2013) R488–R503.
[36] S. Nielsen, C.L. Chou, D. Marples, E.I. Christensen, B.K. Kishore, M.A. Knepper, Vasopressin increases water permeability of kidney collecting duct by inducing translocation of aquaporin-cd water channels to plasma-membrane, Proc. Natl. Acad. Sci. U. S. A. 92 (1995) 1013–1017.
[37] T. Yamamoto, S. Sasaki, K. Fushimi, K. Ishibashi, E. Yaoita, K. Kawasaki, F. Marumo, I. Kihara, Vasopressin increases AQP-CD water channel in apical membrane of collecting duct cells in Brattleboro rats, Am. J. Physiol. 268 (1995) C1546–C1551.
[38] S.R. Digiovanni, S. Nielsen, E.I. Christensen, M.A. Knepper, Regulation of collecting duct water channel expression by vasopressin in Brattleboro rat, Proc. Natl. Acad. Sci. U. S. A. 91 (1994) 8984–8988.
[39] K. Fushimi, S. Uchida, Y. Hara, Y. Hirata, F. Marumo, S. Sasaki, Cloning and expression of apical membrane water channel of rat-kidney collecting tubule, Nature 361 (1993) 549–552.
[40] T.H. Ma, Y.L. Song, B.X. Yang, A. Gillespie, E.J. Carlson, C.J. Epstein, A.S. Verkman, Nephrogenic diabetes insipidus in mice lacking aquaporin-3 water channels, Proc. Natl. Acad. Sci. U. S. A. 97 (2000) 4386–4391.
[41] T. Ma, B. Yang, A. Gillespie, E.J. Carlson, C.J. Epstein, A.S. Verkman, Generation and phenotype of a transgenic knockout mouse lacking the mercurial-insensitive water channel aquaporin-4, J. Clin. Invest. 100 (1997) 957–962.
[42] F. Drees, A. Reilein, W.J. Nelson, Cell-adhesion assays: fabrication of an E-cadherin substratum and isolation of lateral and Basal membrane patches, Methods Mol. Biol. 294 (2005) 303–320.
[43] N. Borghi, M. Lowndes, V. Maruthamuthu, M.L. Gardel, W.J. Nelson, Regulation of cell motile behavior by crosstalk between cadherin- and integrin-mediated adhesions, Proc. Natl. Acad. Sci. U. S. A. 107 (2010) 13324–13329.
[44] S.J. Hunt, W.J. Nelson, Fabrication of a dual substrate display to test roles of cell adhesion proteins in vesicle targeting to plasma membrane domains, FEBS Lett. 581 (2007) 4539–4543.
[45] D.L. Kolin, D. Ronis, P.W. Wiseman, k-Space image correlation spectroscopy: a method for accurate transport measurements independent of fluorophore photophysics, Biophys. J. 91 (2006) 3061–3075.
[46] E.C. Arnspang, J. Schwartzentruber, M.P. Clausen, P.W. Wiseman, B.C. Lagerholm, Bridging the gap between single molecule and ensemble methods for measuring lateral dynamics in the plasma membrane, PLoS One 9 (6) (2014 Jun 3) e97671, http://dx.doi.org/10.1371/journal.pone.0097671 eCollection 2014.
[47] E.C. Arnspang, J.S. Koffman, S. Marlar, P.W. Wiseman, L.N. Nejsum, Easy measurement of diffusion coefficients of EGFP-tagged plasma membrane proteins using k-space image correlation spectroscopy, J. Vis. Exp. (87) (2014 May 10), http://dx.doi.org/10.3791/51074.
[48] C.R. Gaush, W.L. Hard, T.F. Smith, Characterization of an established line of canine kidney cells (MDCK), Proc. Soc. Exp. Biol. Med. 122 (1966) 931–935.
[49] D. Louvard, Apical membrane aminopeptidase appears at site of cell–cell contact in cultured kidney epithelial-cells, Proc. Natl. Acad. Sci. Biol. 77 (1980) 4132–4136.
[50] E.C. Arnspang, S. Sundbye, W.J. Nelson, L.N. Nejsum, Aquaporin-3 and aquaporin-4 are sorted differently and separately in the trans-Golgi network, PLoS One 8 (2013) e73977.
[51] C.S. Furman, D.A. Gorelick-Feldman, K.G. Davidson, T. Yasumura, J.D. Neely, P. Agre, J. E. Rash, Aquaporin-4 square array assembly: opposing actions of M1 and M23 isoforms, Proc. Natl. Acad. Sci. U. S. A. 100 (2003) 13609–13614.
[52] C.A. Schneider, W.S. Rasband, K.W. Eliceiri, NIH Image to ImageJ: 25 years of image analysis, Nat. Methods 9 (2012) 671–675.
[53] D.M. Owen, D. Williamson, C. Rentero, K. Gaus, Quantitative microscopy: protein dynamics and membrane organisation, Traffic 10 (2009) 962–971.

[54] A.J. Jesaitis, J. Yguerabide, The lateral mobility of the (Na+, K+)-dependent atpase in Madin–Darby canine kidney-cells, J. Cell Biol. 102 (1986) 1256–1263.
[55] J.M. Crane, A.S. Verkman, Long-range nonanomalous diffusion of quantum dot-labeled aquaporin-1 water channels in the cell plasma membrane, Biophys. J. 94 (2008) 702–713.
[56] S.N. Ahmed, D.A. Brown, E. London, On the origin of sphingolipid/cholesterol-rich detergent-insoluble cell membranes: physiological concentrations of cholesterol and sphingolipid induce formation of a detergent-insoluble, liquid-ordered lipid phase in model membranes, Biochemistry 36 (1997) 10944–10953.
[57] E. London, D.A. Brown, Insolubility of lipids in triton X-100: physical origin and relationship to sphingolipid/cholesterol membrane domains (rafts), Biochim. Biophys. Acta 1508 (2000) 182–195.
[58] K. Simons, D. Toomre, Lipid rafts and signal transduction, Nat. Rev. Mol. Cell Biol. 1 (2000) 31–39.
[59] H.T. He, A. Lellouch, D. Marguet, Lipid rafts and the initiation of T cell receptor signaling, Semin. Immunol. 17 (2005) 23–33.
[60] L.J. Foster, C.L. De Hoog, M. Mann, Unbiased quantitative proteomics of lipid rafts reveals high specificity for signaling factors, Proc. Natl. Acad. Sci. U. S. A. 100 (2003) 5813–5818.
[61] F. Lafont, P. Verkade, T. Galli, C. Wimmer, D. Louvard, K. Simons, Raft association of SNAP receptors acting in apical trafficking in Madin–Darby canine kidney cells, Proc. Natl. Acad. Sci. U. S. A. 96 (1999) 3734–3738.
[62] E. Ikonen, Roles of lipid rafts in membrane transport, Curr. Opin. Cell Biol. 13 (2001) 470–477.
[63] P. Lajoie, I.R. Nabi, Lipid rafts, caveolae, and their endocytosis, Int. Rev. Cell Mol. Biol. 282 (2010) 135–163.
[64] L. Rajendran, K. Simons, Lipid rafts and membrane dynamics, J. Cell Sci. 118 (2005) 1099–1102.
[65] J.S. Goodwin, K.R. Drake, C.L. Remmert, A.K. Kenworthy, Ras diffusion is sensitive to plasma membrane viscosity, Biophys. J. 89 (2005) 1398–1410.
[66] K. Bacia, D. Scherfeld, N. Kahya, P. Schwille, Fluorescence correlation spectroscopy relates rafts in model and native membranes, Biophys. J. 87 (2004) 1034–1043.
[67] J.H. Tong, M.M. Briggs, D. Mlaver, A. Vidal, T.J. McIntosh, Sorting of lens aquaporins and connexins into raft and nonraft bilayers: role of protein homo-oligomerization, Biophys. J. 97 (2009) 2493–2502.
[68] H. Kobayashi, H. Yokoo, T. Yanagita, S. Satoh, B. Kis, M. Deli, M. Niwa, A. Wada, Induction of aquaporin 1 by dexamethasone in lipid rafts in immortalized brain microvascular endothelial cells, Brain Res. 1123 (2006) 12–19.
[69] P. Palestini, C. Calvi, E. Conforti, R. Daffara, L. Botto, G. Miserocchi, Compositional changes in lipid microdomains of air–blood barrier plasma membranes in pulmonary interstitial edema, J. Appl. Physiol. 95 (2003) 1446–1452.
[70] X. Zheng, W. Bollinger Bollag, Aquaporin 3 colocates with phospholipase d2 in caveolin-rich membrane microdomains and is downregulated upon keratinocyte differentiation, J. Investig. Dermatol. 121 (2003) 1487–1495.
[71] G. Noel, D.K. Tham, H. Moukhles, Interdependence of laminin-mediated clustering of lipid rafts and the dystrophin complex in astrocytes, J. Biol. Chem. 284 (2009) 19694–19704.
[72] Y. Ishikawa, Z. Yuan, N. Inoue, M.T. Skowronski, Y. Nakae, M. Shono, G. Cho, M. Yasui, P. Agre, S. Nielsen, Identification of AQP5 in lipid rafts and its translocation to apical membranes by activation of M3 mAChRs in interlobular ducts of rat parotid gland, Am. J. Physiol. Cell Physiol. 289 (2005) C1303–C1311.
[73] J. Kwik, S. Boyle, D. Fooksman, L. Margolis, M.P. Sheetz, M. Edidin, Membrane cholesterol, lateral mobility, and the phosphatidylinositol 4,5-bisphosphate-dependent organization of cell actin, Proc. Natl. Acad. Sci. U. S. A. 100 (2003) 13964–13969.
[74] S.Y. Nishimura, M. Vrljic, L.O. Klein, H.M. McConnell, W.E. Moerner, Cholesterol depletion induces solid-like regions in the plasma membrane, Biophys. J. 90 (2006) 927–938.
[75] Y. Chen, B.C. Lagerholm, B. Yang, K. Jacobson, Methods to measure the lateral diffusion of membrane lipids and proteins, Methods 39 (2006) 147–153.
[76] O. Lieleg, M. Lopez-Garcia, C. Semmrich, J. Auernheimer, H. Kessler, A.R. Bausch, Specific integrin labeling in living cells using functionalized nanocrystals, Small 3 (2007) 1560–1565.
[77] J.M. Crane, A.N. Van Hoek, W.R. Skach, A.S. Verkman, Aquaporin-4 dynamics in orthogonal arrays in live cells visualized by quantum dot single particle tracking, Mol. Biol. Cell 19 (2008) 3369–3378.